The 8th European Congress on Computational Methods in Applied Sciences and Engineering
ECCOMAS Congress 2022
5-9 June 2022, Oslo, Norway

TANGENTIAL DIFFERENTIAL CALCULUS FOR CURVED, LINEAR KIRCHHOFF BEAMS WITH SYSTEMATIC CONVERGENCE STUDIES

MICHAEL W. KAISER[1] AND THOMAS-PETER FRIES[1]

[1] Institute of Structural Analysis
Graz University of Technology
Lessingstraße 25-II, 8010 Graz, Austria
e-mail: michael.kaiser@tugraz.at, fries@tugraz.at, ifb.tugraz.at

Key words: Kirchhoff beam, TDC, FEM, convergence studies

Abstract. We propose a reformulation of linear Kirchhoff beams in two dimensions based on the tangential differential calculus (TDC). The rotation-free formulation of the Kirchhoff beam is classically based on curvilinear coordinates. However, for general applications in engineering and sciences that take place on curved geometries embedded in a higher-dimensional space, the tangential differential calculus enables a formulation independent of curvilinear coordinates and, hence, is suitable also for implicitly defined geometries. The geometry and differential operators are formulated in global Cartesian coordinates related to the embedding space. Isogeometric analysis (IGA) is employed for the generation of shape functions in the numerical analysis because Kirchhoff kinematics require C_1-continuous shape functions. The boundary conditions are enforced using Lagrange multipliers. We emphasize systematic convergence studies for established and new test cases by investigating residual errors. Therefore, the approximated solution obtained by the FEM is inserted into the strong form of the governing equations in a post-processing step. The error is then integrated over the domain in an L_2-sense. For sufficiently smooth physical fields, higher-order convergence rates in the residual errors are achieved. For classical benchmark test cases with known analytical solutions, we also confirm optimal convergence rates in the displacements.

1 INTRODUCTION

Kirchhoff beams, also known as curved Euler-Bernoulli beams, are thin curved beams which fulfill the so called Euler-Bernoulli or Kirchhoff assumptions. These are that the cross section of the beam remains plane and orthogonal to the beam axis after the deformation of the beam. The Kirchhoff constraint states that shear deformations are vanishing in this model, e.g. [1, 2]. Note that a planar Kirchhoff beam is a one-dimensional beam embedded in a two-dimensional plane and a spatial Kirchhoff beam is a one-dimensional structure in $\mathbb{R}^3$. For this work, one-dimensional curved beams in a two dimensional plane are investigated. In the classical formulation, a local curvilinear coordinate system is used. The geometry of the beam depends on a parametrization which is generally not unique. That is, the same curved beam geometry can be described by infinitely many maps. Within this geometry description co- and contravariant base vectors occur naturally. For mathematical operations on this domain, some additional quantities and operators, e.g., Christoffel symbols, are necessary. Components of tensor quantities, e.g., load vectors and stress tensors, are expressed in co- or contravariant components. Linear curved Euler-Bernoulli beams based on curvilinear coordinates are described in [3] and non-linear ones in [4, 5]. In shell mechanics, the analogy to Kirchhoff beams are Kirchhoff-Love shells. In the classical description of Kirchhoff-Love shells, curvilinear coordinates are used for the definition of the two-dimensional middle surface of the shell and the mechanical tensors [6, 7].

We emphasise a reformulation of Kirchhoff beams in a plane where the geometric quantities, mathematical operators and mechanical tensors are described in global Cartesian coordinates. This approach is known as tangential differential calculus [8, 9]. It has been used in structural mechanics for shells [10, 11, 12, 13], for spatial beams [1], membranes [14], and ropes and membranes [15]. TDC can also be applied in fluid mechanics, e.g. [16, 17]. This work is related to the reformulation of the Kirchhoff-Love shell in terms of TDC [12]. The main advantage of using a TDC-based model instead of a classical formulation based on curvilinear coordinates is that the description is independent of a parametrization. Therefore, it is also possible to define the geometry implicitly, that is, based on level-sets. Then, co- and contravariant bases and certain quantities, such as, e.g., Christoffel symbols, are not necessary. A TDC-based formulation is more general because of these aspects.

In a TDC-based formulation for a Kirchhoff beam, the centre axis of the beam is a one dimensional manifold embedded in a two-dimensional space $\mathbb{R}^2$. For the curved, planar Kirchhoff beam based on TDC the vectors describing geometric and mechanical quantities are 2×1 and second-order tensors have a 2×2 - coefficient matrix. The base vectors of these vectors and tensors are the global Cartesian base vectors $\boldsymbol{x} = \boldsymbol{e}_1$ and $\boldsymbol{y} = \boldsymbol{e}_2$ which are unit vectors. For the numerical results in this contribution a parametrized mapping is used to discretize the weak form of the BVP. Test and trial functions must fulfill C_1-continuity because of the kinematics which results from the Kirchhoff constraints. Therefore, isogemetric analysis (IGA) is used where the test and trial functions are B-splines (NURBS) [18, 19]. The approximated solution is used together with the strong form of the governing equations of this BVP to calculate the so called residual error (also denoted as strong form error) in the L_2-norm.

An outline of this paper is as follows: In section 2, tangential differential calculus is introduced; in section 3 the mechanical model of the Kirchhoff beam is described, followed by some aspects of the implementation in section 4, and in section 5 numerical test cases and results are shown. Finally this paper closes with a conclusion.

2 TANGENTIAL DIFFERENTIAL CALCULUS

Partial differential equations (PDEs) on surfaces can be modelled using tangential differential calculus (TDC) [20]. A manifold Γ with dimension q is embedded in a d-dimensional space $\mathbb{R}^d$. The difference $d - q$ is the codimension of Γ. For the Kirchhoff beam $q = 1$ and $d = 2$, so, a 1-dimensional manifold is embedded in $\mathbb{R}^2$. Geometry and differential operators with respect to global Cartesian coordinates can then be defined using TDC on such manifolds. We restrict the definitions here to the case of $q = 1$ and $d = 2$. However, the concepts are easily extended to other situations, e.g., with $q = 2$ and $d = 3$ for shells [12, 13]. Figure 1 shows a 1-dimensional manifold embedded in $\mathbb{R}^2$. In Figure 1(a) the normal and co-normal vectors are shown and further the two possible types of geometry definitions are visualized: In Figure 1(b) an explicitly defined geometry is depicted and in Figure 1(c) an implicitly defined geometry is shown.

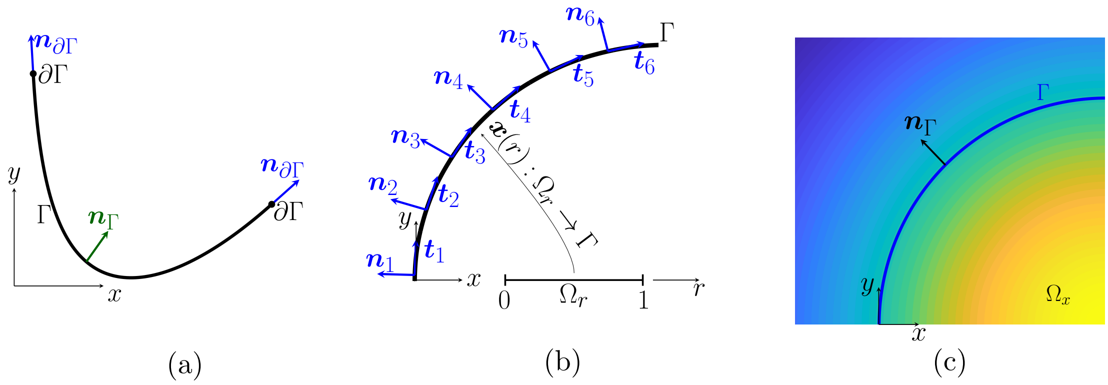

Figure 1: (a) 1-dimensional manifold Γ embedded in $\mathbb{R}^2$ with normal vector $\boldsymbol{n}_\Gamma$, boundary points $\partial\Gamma$, and co-normal vectors $\boldsymbol{n}_{\partial\Gamma}$; (b) explicit and (c) implicit geometry definition of Γ.

One possibility to define the manifold describing the central axis of the Kirchhoff beam is through a parametrization, see Figure 1(b). This is a bijective mapping

$$\boldsymbol{x}(\boldsymbol{r}) : \Omega_r \to \Gamma \tag{1}$$

from the parameter space $\Omega_r \subset \mathbb{R}^1$ to the real domain $\Gamma \subset \mathbb{R}^2$. Based on the parametrization, a Jacobi matrix $\mathbf{J}$ can be defined with dimension 2×1 which is a tangential vector to Γ.

$$\mathbf{J}(\boldsymbol{r}) = \nabla_r \boldsymbol{x}(\boldsymbol{r}) = \frac{\partial \boldsymbol{x}}{\partial \boldsymbol{r}} = \begin{pmatrix} t_1^* \\ t_2^* \end{pmatrix} = \boldsymbol{t}_\Gamma^* \tag{2}$$

where * indicates that the vector is not normed. The normed tangential vector is then

$$\boldsymbol{t}_\Gamma = \frac{\boldsymbol{t}_\Gamma^*}{\|\boldsymbol{t}_\Gamma^*\|} = \begin{pmatrix} t_1 \\ t_2 \end{pmatrix}. \tag{3}$$

The normed normal vector follows as

$$\boldsymbol{n}_\Gamma = \begin{pmatrix} -t_2 \\ t_1 \end{pmatrix}. \tag{4}$$

The first fundamental form is defined as

$$\mathbf{G} = \mathbf{J}^{\mathrm{T}} \cdot \mathbf{J} \tag{5}$$

which is a $q \times q$ quantity. Later the Moore-Penrose-(pseudo)-inverse is used. It is defined as

$$\mathbf{Q} = \mathbf{J}^{+} = \mathbf{J} \cdot \mathbf{G}^{-1}. \tag{6}$$

It is also possible to describe the manifold implicitly using the level-set method, see Figure 1(c). A level-set function $\phi(\boldsymbol{x}) : \mathbb{R}^2 \to \mathbb{R}$ with $\boldsymbol{x} \in \Omega_{\boldsymbol{x}} \subset \mathbb{R}^2$ describes the beam implicitly via the zero-isoline as

$$\Gamma = \left\{ \boldsymbol{x} \in \Omega_{\boldsymbol{x}} : \phi(\boldsymbol{x}) = 0 \right\}. \tag{7}$$

The unit normal vector is then defined as

$$\boldsymbol{n}_\Gamma = \frac{\nabla_{\boldsymbol{x}} \phi}{\|\nabla_{\boldsymbol{x}} \phi\|} \tag{8}$$

where $\nabla_x \phi$ is the gradient of the level-set function.

To map an arbitrary vector to the tangent space $T_x\Gamma$, the projector

$$\mathbf{P} = \mathbf{I} - \boldsymbol{n}_\Gamma \otimes \boldsymbol{n}_\Gamma \tag{9}$$

is introduced. The projection of the arbitrary vector-field $\boldsymbol{v} : \Gamma \to \mathbb{R}^2$ onto the tangent space is defined by $\boldsymbol{v}_t = \mathbf{P} \cdot \boldsymbol{v} \in T_x\Gamma$. Important properties of the projector are: The projection of a tangential second-order tensor $\boldsymbol{A}_t = \mathbf{P} \cdot \boldsymbol{A}_t \cdot \mathbf{P}$ is this tensor itself and because the projector maps onto the tangent space, there follows $\mathbf{P} \cdot \boldsymbol{n}_\Gamma = \mathbf{0}$. Further, $\mathbf{P}$ is symmetric, i.e., $\mathbf{P} = \mathbf{P}^\mathrm{T}$ and idempotent, i.e., $\mathbf{P} \cdot \mathbf{P} = \mathbf{P}$.

2.1 Tangential gradient of scalar functions

The gradient of a scalar function $f : \Gamma \to \mathbb{R}$ on the parametric manifold is defined as

$$\nabla_\Gamma f = \mathbf{Q} \cdot \nabla_{\boldsymbol{r}} f = \begin{bmatrix} \partial_x^\Gamma f \\ \partial_y^\Gamma f \end{bmatrix}. \tag{10}$$

with $\nabla_{\boldsymbol{r}}$ being the gradient with respect to the reference coordinates. Important properties are that $\mathbf{P} \cdot \nabla_\Gamma f = \nabla_\Gamma f$ and $\nabla_\Gamma f \cdot \boldsymbol{n}_\Gamma = 0$.

For the implicitly defined manifold, the gradient of a scalar function $f(\boldsymbol{x})$ with $\boldsymbol{x} \in \mathbb{R}^2$ is the projection of the classical gradient onto the tangent space

$$\nabla_\Gamma f = \mathbf{P} \cdot \nabla_{\boldsymbol{x}} f. \tag{11}$$

2.2 Tangential gradients of vector-valued functions

For a vector-valued function $\boldsymbol{u}(\boldsymbol{x}) = (u \quad v)^\mathrm{T} : \Gamma \to \mathbb{R}^2$ there are two gradient operators to distinguish. The *directional* gradient of $\boldsymbol{u}$ is defined as

$$\nabla_\Gamma^{\mathrm{dir}} \boldsymbol{u}(\boldsymbol{x}) = \begin{bmatrix} (\nabla_\Gamma u)^\mathrm{T} \\ (\nabla_\Gamma v)^\mathrm{T} \end{bmatrix} = \begin{bmatrix} \partial_x^\Gamma u & \partial_y^\Gamma u \\ \partial_x^\Gamma v & \partial_y^\Gamma v \end{bmatrix}. \tag{12}$$

Generally, the directional gradients of vector-valued functions are not in the tangent space. The projection of this directional gradient onto the tangent space leads to the *covariant* gradient of a vector-valued function, i.e.,

$$\nabla_\Gamma^{\mathrm{cov}} \boldsymbol{u}(\boldsymbol{x}) = \mathbf{P} \cdot \nabla_\Gamma^{\mathrm{dir}} \boldsymbol{u}(\boldsymbol{x}). \tag{13}$$

The following important relations and properties are noted: $\nabla_\Gamma^{\mathrm{dir}} \boldsymbol{u} \neq \left(\nabla_\Gamma^{\mathrm{dir}} \boldsymbol{u}\right)^\mathrm{T}$, $\nabla_\Gamma^{\mathrm{cov}} \boldsymbol{u} \neq \left(\nabla_\Gamma^{\mathrm{cov}} \boldsymbol{u}\right)^\mathrm{T}$, $\nabla_\Gamma^{\mathrm{dir}} \boldsymbol{u} \cdot \boldsymbol{n}_\Gamma = \mathbf{0}$, $\nabla_\Gamma^{\mathrm{cov}} \boldsymbol{u} \cdot \boldsymbol{n}_\Gamma = \mathbf{0}$, and $\nabla_\Gamma^{\mathrm{dir}} \boldsymbol{u} \cdot \mathbf{P} = \nabla_\Gamma^{\mathrm{dir}} \boldsymbol{u}$.

2.3 Tangential gradients of tensor functions

For a second-order tensor function $\boldsymbol{A}(\boldsymbol{x}) : \Gamma \to \mathbb{R}^2$, there are again directional and covariant gradient operators to distinguish. The *directional* gradient of $\boldsymbol{A}$ with respect to x_i is defined as

$$\nabla^{\text{dir}}_{\Gamma,i}\boldsymbol{A}(\boldsymbol{x}) = \frac{\partial \boldsymbol{A}}{\partial^{\Gamma}_{x_i}} = \begin{bmatrix} \partial^{\Gamma}_{x_i} A_{11} & \partial^{\Gamma}_{x_i} A_{12} \\ \partial^{\Gamma}_{x_i} A_{21} & \partial^{\Gamma}_{x_i} A_{22} \end{bmatrix} \tag{14}$$

and the *covariant* gradient of $\boldsymbol{A}$ is obtained by

$$\nabla^{\text{cov}}_{\Gamma,i}\boldsymbol{A}(\boldsymbol{x}) = \mathbf{P} \cdot \nabla^{\text{dir}}_{\Gamma,i}\boldsymbol{A} \cdot \mathbf{P}. \tag{15}$$

2.4 Curvature

The Weingarten map [8, 17] is related to the second fundamental form in classical differential geometry and therefore to curvature. It is defined as

$$\mathbf{H} = \nabla^{\text{dir}}_{\Gamma}\boldsymbol{n}_{\Gamma} = \nabla^{\text{cov}}_{\Gamma}\boldsymbol{n}_{\Gamma} \tag{16}$$

and a symmetric in-plane tensor. Therefore, a 1-dimensional manifold embedded in $\mathbb{R}^2$ has one eigenvalue which is zero and the other one is the curvature of the manifold, i.e., $\varkappa = -\text{eig}(\boldsymbol{H})$.

2.5 Tangential divergence operators and divergence theorems

Tangential divergence operators for vector-valued functions $\boldsymbol{u}$ and second-order tensor functions $\boldsymbol{A}$ are used in the equations describing the mechanical behaviour of the Kirchhoff beam later. To derive the weak form of the PDE starting from the strong form, integral theorems are necessary. The tangential divergence operator for a vector-valued function $\boldsymbol{u}$ is defined by

$$\text{div}_{\Gamma}\boldsymbol{u} = \text{tr}\big(\nabla^{\text{dir}}_{\Gamma}\big) = \text{tr}\big(\nabla^{\text{cov}}_{\Gamma}\big) \tag{17}$$

and for a second-order tensor function, the tangential divergence is defined by

$$\text{div}_{\Gamma}\boldsymbol{A} = \begin{bmatrix} \text{div}_{\Gamma}\big[\boldsymbol{A}\big]_{1i} \\ \text{div}_{\Gamma}\big[\boldsymbol{A}\big]_{2i} \end{bmatrix} = \begin{bmatrix} \text{div}_{\Gamma}\big[A_{11} \quad A_{12}\big] \\ \text{div}_{\Gamma}\big[A_{21} \quad A_{22}\big] \end{bmatrix}. \tag{18}$$

The divergence theorem used in TDC is defined

- for a scalar function f and a vector function $\boldsymbol{u}$ as:

$$\int_{\Gamma} f \cdot \text{div}_{\Gamma}\boldsymbol{u}\,\text{d}\Gamma = -\int_{\Gamma} \nabla_{\Gamma} f \cdot \boldsymbol{u}\,\text{d}\Gamma + \int_{\Gamma} \varkappa f(\boldsymbol{u} \cdot \boldsymbol{n}_{\Gamma})\,\text{d}\Gamma + \int_{\partial\Gamma} f\boldsymbol{u} \cdot \boldsymbol{n}_{\partial\Gamma}\,\text{d}s. \tag{19}$$

- for a vector function $\boldsymbol{u}$ and a second-order tensor function $\boldsymbol{A}$ as:

$$\int_{\Gamma} \boldsymbol{u} \cdot \text{div}_{\Gamma}\boldsymbol{A}\,\text{d}\Gamma = -\int_{\Gamma} \nabla^{\text{dir}}_{\Gamma}\boldsymbol{u} : \boldsymbol{A}\,\text{d}\Gamma + \int_{\Gamma} \varkappa\boldsymbol{u} \cdot (\boldsymbol{A} \cdot \boldsymbol{n}_{\Gamma})\,\text{d}\Gamma + \int_{\partial\Gamma} \boldsymbol{u} \cdot (\boldsymbol{A} \cdot \boldsymbol{n}_{\partial\Gamma})\,\text{d}s. \tag{20}$$

The terms including curvature $\varkappa$ vanish if the vector $\boldsymbol{u}$ is tangential in equation (19) and if the tensor $\boldsymbol{A}$ is tangential in equation (20). The double dot product is defined as $\nabla^{\text{dir}}_{\Gamma}\boldsymbol{u} : \boldsymbol{A} = \text{tr}\big(\nabla^{\text{dir}}_{\Gamma}\boldsymbol{u} \cdot \boldsymbol{A}^{\text{T}}\big)$ and further, there holds $\nabla^{\text{dir}}_{\Gamma}\boldsymbol{u} : \boldsymbol{A}_t = \nabla^{\text{cov}}_{\Gamma}\boldsymbol{u} : \boldsymbol{A}_t$ if $\boldsymbol{A}_t$ is an in-plane tensor.

3 KIRCHHOFF BEAMS

The derivation of the governing equations of the linear Kirchhoff beam in a two-dimensional plane based on TDC is shown in this section. The deformations are infinitesimal, i.e., the reference and actual configurations of the beam are indistinguishable. Therefore, equilibrium can be formulated in the undeformed configuration. A linear-elastic material is assumed which fulfils Hooke's law. The considered beams are supposed to be thin such that the Kirchhoff (Bernoulli) assumptions can be applied and shear strain is neglected. As general in structural mechanics we distinguish the fields of kinematics, constitutive relations (material) and equilibrium in the derivation.

3.1 Kinematics

The displacement field is described by the vector $\boldsymbol{u} = (u \quad v)^{\mathrm{T}}$. To describe the deformation induced by bending actions, the difference vector $\boldsymbol{w}$ is introduced as

$$\boldsymbol{w} = -\left(\nabla_{\Gamma}^{\mathrm{dir}} \boldsymbol{u}\right)^{\mathrm{T}} = \mathbf{H} \cdot \boldsymbol{u} - \nabla_{\Gamma}\left(\boldsymbol{u} \cdot \boldsymbol{n}_{\Gamma}\right) \tag{21}$$

Figure 2 shows the kinematic relations for the linear Kirchhoff beam.

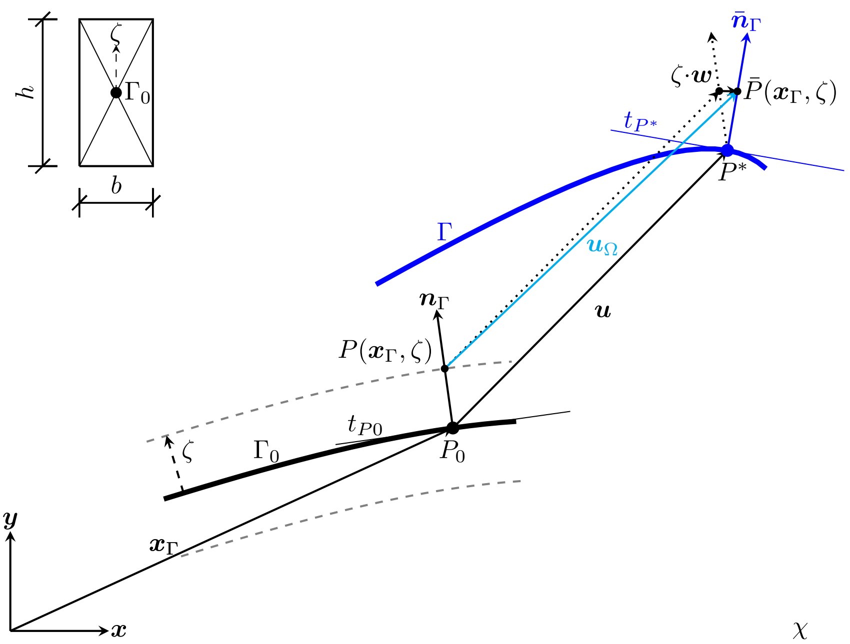

Figure 2: Kinematic relations for the linear Kirchhoff beam.

Γ_0 denotes the beam's centre axis in the initial configuration. The dark blue line Γ is this axis after deformation. A point P within the beam's cross section has a distance ζ normal to the centre axis. The cross section is constant over the beam-length. The vector $\boldsymbol{u}$ describes the deformation of the beam's axis. The strain tensor is built up using components for membrane and bending action as

$$\boldsymbol{\varepsilon}_{\Gamma}^{\mathrm{dir}} = \boldsymbol{\varepsilon}_{\Gamma,M}^{\mathrm{dir}}(\boldsymbol{u}) + \zeta \boldsymbol{\varepsilon}_{\Gamma,B}^{\mathrm{dir}}(\boldsymbol{w}). \tag{22}$$

There, the membrane strain tensor is defined by

$$\boldsymbol{\varepsilon}_{\Gamma,M}^{\mathrm{dir}}(\boldsymbol{u}) = \begin{bmatrix} \boldsymbol{u}_{,x}^{\mathrm{dir}} & \frac{1}{2}(\boldsymbol{u}_{,x}^{\mathrm{dir}} + \boldsymbol{u}_{,y}^{\mathrm{dir}}) \\ \text{sym.} & \boldsymbol{u}_{,y}^{\mathrm{dir}} \end{bmatrix} \tag{23}$$

and the bending part is expressed as a function of $\boldsymbol{u}$ as

$$\boldsymbol{\varepsilon}_{\Gamma,B}^{\mathrm{dir}}(\boldsymbol{u}) = -\begin{bmatrix} \boldsymbol{u}_{,xx}^{\mathrm{dir}}\boldsymbol{n}_\Gamma & \frac{1}{2}(\boldsymbol{u}_{,xy}^{\mathrm{dir}} + \boldsymbol{u}_{,yx}^{\mathrm{dir}})\boldsymbol{n}_\Gamma \\ \text{sym.} & \boldsymbol{u}_{,yy}^{\mathrm{dir}}\boldsymbol{n}_\Gamma \end{bmatrix}. \tag{24}$$

The mixed terms in equation (24) cannot be summed up because the directional gradient operator is not symmetric. However, the resulting strain tensor itself is a symmetric tensor.

3.2 Constitutive relations

As already described above, linear-elastic material behaviour according to Hooke's law is assumed. The cross section is constant over the beam's length. This means that a pre-integration of the strain tensor is possible which leads to second-order tensors for normal forces and bending moments. The bending moment tensor follows as

$$\mathbf{M}_\Gamma(\boldsymbol{u}) = \mathbf{P} \cdot \mathbf{M}_\Gamma^{\mathrm{dir}} \cdot \mathbf{P} = EI \cdot \mathbf{P} \cdot \boldsymbol{\varepsilon}_{\Gamma,B}^{\mathrm{dir}} \cdot \mathbf{P} \tag{25}$$

and the effective normal force tensor as

$$\tilde{\mathbf{N}}_\Gamma(\boldsymbol{u}) = EA \cdot \mathbf{P} \cdot \boldsymbol{\varepsilon}_{\Gamma,M}^{\mathrm{dir}} \cdot \mathbf{P}. \tag{26}$$

To get physical normal forces it is necessary to consider the beam's curvature and bending moments. The real normal force is denoted by

$$\mathbf{N}_\Gamma^{\mathrm{real}} = \tilde{\mathbf{N}}_\Gamma + \mathbf{H} \cdot \mathbf{M}_\Gamma \tag{27}$$

which is the physically occurring internal normal force in the beam's centre line. Further scalar values for the normal forces and bending moments are determined. These are obtained as the non-zero eigenvalues of the tensors $\tilde{\mathbf{N}}_\Gamma$ and $\mathbf{M}_\Gamma$. Therefore, $\tilde{\mathcal{N}} = \mathrm{tr}(\tilde{\mathbf{N}}_\Gamma)$ and $\mathcal{M} = \mathrm{tr}(\mathbf{M}_\Gamma)$ are the scalar-valued internal normal forces and moments respectively.

3.3 Equilibrium

Using the quantities defined above, the equations for equilibrium are obtained. The governing partial differential equation (PDE) in strong form is expressed in terms of TDC as

$$\mathrm{div}_\Gamma \boldsymbol{N}_\Gamma^{\mathrm{real}} + \boldsymbol{n}_\Gamma \cdot \mathrm{div}_\Gamma(\mathbf{P} \cdot \mathrm{div}_\Gamma \boldsymbol{M}_\Gamma) + \mathbf{H} \cdot \mathrm{div}_\Gamma \boldsymbol{M}_\Gamma = -\boldsymbol{f}. \tag{28}$$

It is important to note, that in contrast to classical definitions, the strong form (28) does not rely on any curvilinear coordinates and may, hence, also be used for implicitly defined manifolds.

Multiplication of equation (28) with the test function $\boldsymbol{v}$ and integration over the domain Γ leads to the weak form of the PDE expressed as: Find $\boldsymbol{u} \in \mathcal{V}^{KB} : \Gamma \to \mathbb{R}^2$ such that

$$\int_\Gamma \nabla_\Gamma^{\mathrm{dir}} \boldsymbol{v} : \tilde{\boldsymbol{N}}_\Gamma + \boldsymbol{\varepsilon}_{\Gamma,B}^{\mathrm{dir}}(\boldsymbol{v}) : \boldsymbol{M}_\Gamma \,\mathrm{d}\Gamma - \int_{\partial\Gamma} \boldsymbol{v}\big(\tilde{P}_{n_{\partial\Gamma}} \boldsymbol{n}_{\partial\Gamma} + \tilde{P}_{n_\Gamma} \boldsymbol{n}_\Gamma\big) - \omega_{t_{\partial\Gamma}}(\boldsymbol{v}) M_{t_{\partial\Gamma}} \,\mathrm{d}\partial\Gamma = \int_\Gamma \boldsymbol{v}\boldsymbol{f} \,\mathrm{d}\Gamma \quad (29)$$

$\forall\, \boldsymbol{v} \in \mathcal{V}_0^{KB}$.

The corresponding function spaces are defined as:

$$\mathcal{V}^{KB} = \big\{\boldsymbol{u} : \Gamma \to \mathbb{R}^2 \,|\, \boldsymbol{u} \in [\mathcal{H}^1(\Gamma)]^2 : \boldsymbol{u}_{,ji} \cdot \boldsymbol{n}_\Gamma \in [\boldsymbol{\mathcal{L}}^2(\Gamma)]^2\big\} \quad (30)$$

$$\mathcal{V}_0^{KB} = \big\{\boldsymbol{v} \in \mathcal{V}^{KB}(\Gamma) : \boldsymbol{v}|_{\partial\Gamma_D} = \boldsymbol{0}\big\} \quad (31)$$

At the boundary the force in co-normal direction is defined as $\tilde{P}_{n_{\partial\Gamma}} = (\mathbf{N}_\Gamma^{\mathrm{real}} \cdot \boldsymbol{n}_{\partial\Gamma}) \cdot \boldsymbol{n}_{\partial\Gamma}$, in normal direction as $\tilde{P}_{n_\Gamma} = \mathbf{P} \cdot \mathrm{div}_\Gamma(\mathbf{M}_\Gamma) \cdot \boldsymbol{n}_{\partial\Gamma}$. The bending moment is defined as $M_{t_{\partial\Gamma}} = (\mathbf{M}_\Gamma \cdot \boldsymbol{n}_{\partial\Gamma}) \cdot \boldsymbol{n}_{\partial\Gamma}$, and the rotation as $\omega_{t_{\partial\Gamma}} = (\nabla_\Gamma(\boldsymbol{v} \cdot \boldsymbol{n}_\Gamma) - \mathbf{H} \cdot \boldsymbol{v}) \cdot \boldsymbol{n}_{\partial\Gamma}$. The co-normal vector $\boldsymbol{n}_{\partial\Gamma}$ is tangential to Γ at the boundary $\partial\Gamma$, see Figure 1(a).

4 DISCRETIZATION AND IMPLEMENTATIONAL ASPECTS

The mechanical model of the Kirchhoff beam leads to second order derivatives in the weak form. Therefore, in the FEM for Kirchhoff beams, shape functions with C_1-continuity are required. This can be fulfilled using isogeometric analysis (IGA). The splines are the test and trial functions used for the FEM-discretization [18, 19]. The stiffness matrix follows as

$$\boldsymbol{K}_{\mathrm{elem}} = \boldsymbol{K}_{\mathrm{elem,M}} + \boldsymbol{K}_{\mathrm{elem,B}}. \quad (32)$$

The membrane part is defined by

$$\big[\boldsymbol{K}_{\mathrm{elem,M}}\big]_{ij} = \int_\Gamma \sum_{b=1}^{2} P_{ib} \cdot \bar{\boldsymbol{K}}_{bj} \,\mathrm{d}\Gamma \quad \text{with: } \bar{\boldsymbol{K}}_{bj} = \frac{EA}{2}\left[\delta_{bj} \sum_{a=1}^{2} \boldsymbol{N}_{,a} \cdot \boldsymbol{N}_{,a}^{\mathrm{T}} + \boldsymbol{N}_{,j} \cdot \boldsymbol{N}_{,b}^{\mathrm{T}}\right] \quad (33)$$

and the bending part is defined by

$$\big[\boldsymbol{K}_{\mathrm{elem,B}}\big]_{ij} = EI \int_\Gamma n_i \cdot n_j \cdot \tilde{\boldsymbol{K}} \,\mathrm{d}\Gamma \quad \text{with: } \tilde{\boldsymbol{K}} = \sum_{k=1}^{2} \sum_{l=1}^{2} P_{kl} \bigg(\sum_{m=1}^{2} \boldsymbol{N}_{,lm} \boldsymbol{N}_{,mk}^{\mathrm{T}}\bigg) \quad (34)$$

where the $\boldsymbol{N}$ are the B-spline-functions. Dirichlet boundary conditions (BCs) are enforced using Lagrange multipliers. Neumann-BCs are considered at the right hand side as additional terms on the level of the external loading within the domain.

$$\boldsymbol{A} \cdot \boldsymbol{u} = \begin{bmatrix} \boldsymbol{K} & \boldsymbol{C}^{\mathrm{T}} \\ \boldsymbol{C} & \boldsymbol{0} \end{bmatrix} \cdot \begin{bmatrix} \boldsymbol{u} \\ \boldsymbol{\lambda} \end{bmatrix} = \begin{bmatrix} \boldsymbol{f}^* \\ \boldsymbol{b} \end{bmatrix} \quad (35)$$

where $\boldsymbol{f}^*$ are the applied loads including additional terms for Neumann-BCs and $\boldsymbol{b}$ is a vector including the prescribed Dirichlet-BCs.

To verify the accuracy of the FEM approximation, we investigate different errors. For known bench-mark test cases and systems for which analytical solutions can be computed, these reference solutions can be used for an adequate error analysis. In the displacements the optimal convergence rate is $\mathcal{O}(p+1)$ where p is the order of FE-shape functions (here: B-splines). If an analytical solution is not available the error can be measured in the strong form (28) of the PDE. This error is often labelled residual or strong form error $\varepsilon_{\mathrm{SF}}$ and is the summed element-wise relative L_2-error

$$\varepsilon_{\mathrm{SF}} = \varepsilon_{\mathrm{rel,residual}} = \sum_{i=1}^{n_{\mathrm{Elem}}} \varepsilon_{L_2,\mathrm{rel},\tau_i} \tag{36}$$

$$\varepsilon^2_{L_2,\mathrm{rel},\tau_i} = \frac{\int_\Gamma \left(\mathrm{div}_\Gamma \boldsymbol{N}_\Gamma^{\mathrm{real}} + \boldsymbol{n}_\Gamma \cdot \mathrm{div}_\Gamma(\mathbf{P} \cdot \mathrm{div}_\Gamma \boldsymbol{M}_\Gamma) + \mathbf{H} \cdot \mathrm{div}_\Gamma \boldsymbol{M}_\Gamma + \boldsymbol{f}\right)^2 \mathrm{d}\Gamma}{\int_\Gamma \boldsymbol{f}^2 \, \mathrm{d}\Gamma}.$$

Fourth-order derivatives are part of the strong form for Kirchhoff beams. Therefore, the optimal convergence rate for the residual error is $\mathcal{O}(p-3)$ for sufficiently smooth displacement fields [12].

5 NUMERICAL RESULTS

For the TDC-based formulation, several test cases have been investigated. Figure 3 shows the structural system and the solution plots for the deformation $\boldsymbol{u}_\Gamma$, the bending moment, and the normal forces for a sliced arc subjected to a constantly distributed vertical load. The convergence in the displacements and in the residual error are shown in Figure 4 in a double-logarithmic plot over the mesh size h. The expected rates of $\mathcal{O}(p+1)$ in the displacements and $\mathcal{O}(p-3)$ in the residual are confirmed, respectively.

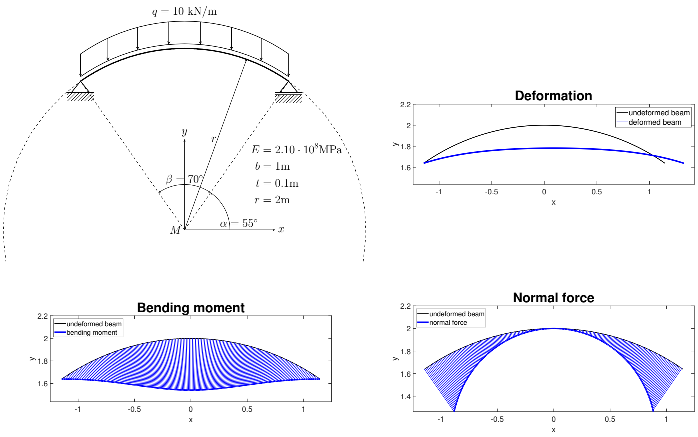

Figure 3: System sketch and results for a sliced arc.

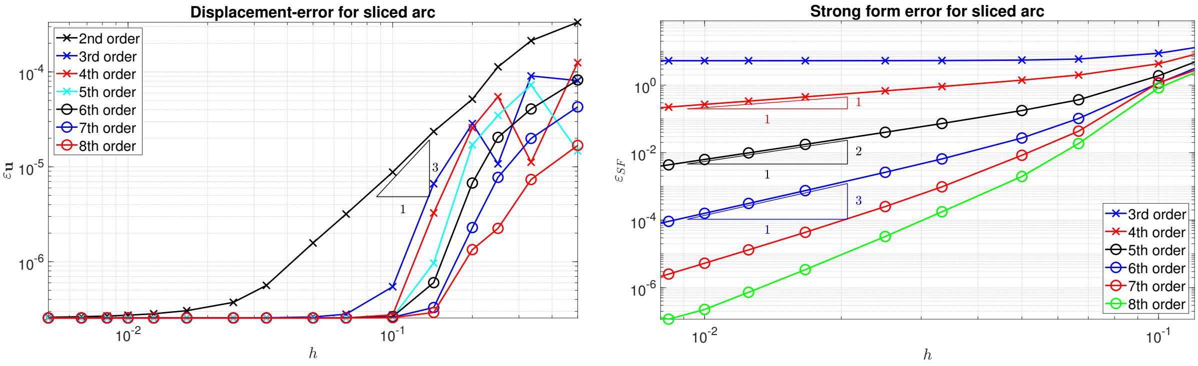

(a) (b)

Figure 4: (a) L_2-error convergence rates for analytical solution of the sliced arc with $\mathcal{O}(p+1)$ and (b) residual error for the same test case with $\mathcal{O}(p-3)$ as expected.

Figure 5 shows the system, the results and the $\varepsilon_{\mathrm{SF}}$-convergence study for a quarter arc subjected to single loads at its free end. Optimal convergence rates are again verified in the shown residual errors.

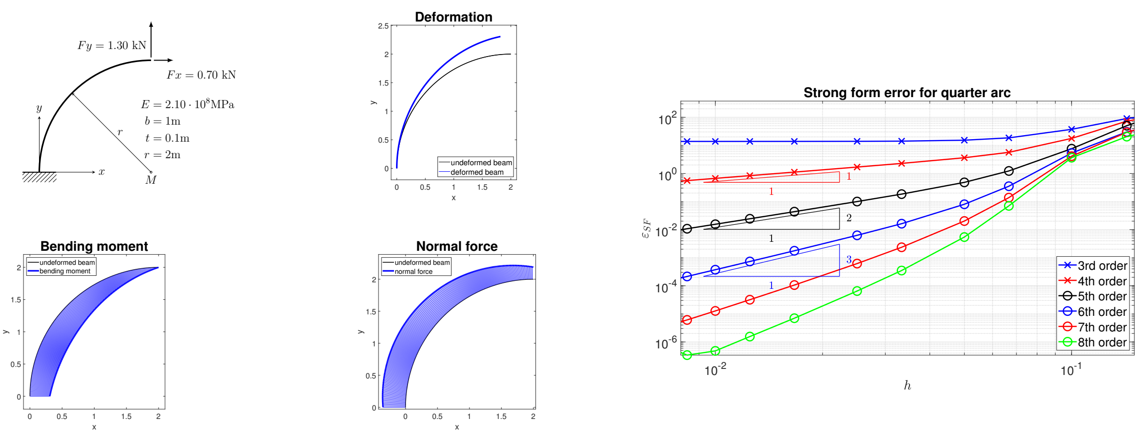

Figure 5: System sketch, results and residual error analysis for a quarter arc.

Figure 6 shows the system, the results and the optimal $\varepsilon_{\mathrm{SF}}$-convergence study for a beam defined by a trigonometric function subjected to distributed loads.

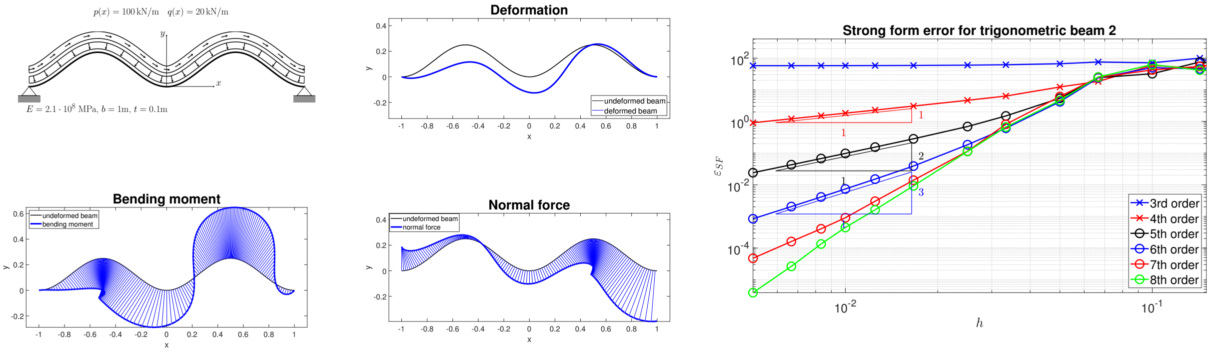

Figure 6: System sketch, results and residual error analysis for a trigonometric beam.

6 CONCLUSION

The Kirchhoff beam has been reformulated based on the TDC which is more general because the beam can be defined parametrically or implicitly. Numerical results for a discretization based on a parametrization using IGA are presented. Optimal convergence rates based on analytical solutions are obtained. A systematic error study based on the residual errors in the L_2-norm is applied to several test cases and shows optimal higher-order convergence rates. This strong form or residual error analysis can be applied even if analytical solutions are not available and, therefore, gives a possibility to verify the accuracy of an approximation also for complicated geometries and loading situations.

7 ACKNOWLEDGEMENT

Discussions with Daniel Schöllhammer about the TDC-based formulation of the Kirchhoff-Love shell and relations to the Kirchhof beam are highly appreciated.

REFERENCES

[1] Hansbo, P., Larson, M. G. and Larsson, K. Variational formulation of curved beams in global coordinates, *Comput. Mech.* (2014) **53**:611–623.

[2] Meier, C., Popp A., and Wall, W. A. Geometrically Exact Finite Element Formulations for Slender Beams: Kirchhoff–Love Theory Versus Simo–Reissner Theory. *Arch. Comput. Methods Eng.* (2017) **26**:163-243

[3] Borković, A., Kovačević, S., Radenković, G., Milovanović, S. and Guzijan-Dilber M. Rotation-free isogeometric analysis of an arbitrarily curved plane Bernoulli–Euler beam. *Comput. Methods Appl. Mech. Engrg.* (2018) **334**:238–267.

[4] Vo, D. and Nanakorn, P. Geometrically nonlinear multi-patch isogeometric analysis of planar curved Euler-Bernoulli beams. *Comput. Methods Appl. Mech. Engrg.* (2020) **366**:113078.

[5] Borković, A., Marussig, B., and Radenković G. Geometrically exact static isogeometric analysis of arbitrarily curved plane Bernoulli–Euler beam, *Thin-Walled Structures* (2022) **170**:108539.

[6] Başar Y. and Krätzig W.B. *Mechanik der Flächentragwerke.* Vieweg & Sohn, Vol. I., (1985).

[7] Kiendl, J., Bletzinger, K.-U., Linhard, J. and Wüchner, R. Isogeometric shell analysis with Kirchhoff-Love elements. *Comput. Methods Appl. Mech. Engrg.* (2009) **198**:3902–3914.

[8] Delfour, M.C. and Zolésio, J.-P. *Shapes and geometries: metrics, analysis, differential calculus, and optimization.* SIAM, Vol. I., (2011).

[9] Dziuk, G. and Elliot, C.M. Finite element methods for surface PDEs. *Acta. Numer.* (2013) **22**:289–396.

[10] Delfour, M.C. and Zolésio, J.-P. A boundary differential equation for thin shells. *J. Differ. Equ.* (1994) **119**:426–449.

[11] Delfour, M.C. and Zolésio, J.-P. Tangential differential equations for dynamical thin shallow shells. *J. Differ. Equ.* (1996) **128**:125-167.

[12] Schöllhammer, D. and Fries, T.-P. Kirchhoff-Love shell theory based on tangential differential calculus. *Comput. Mech.* (2019) **64**:113–131.

[13] Schöllhammer, D. and Fries, T.-P. Reissner-Mindlin shell theory based on tangential differential calculus. *Comp. Methods in Appl. Mech. Engrg.* (2019) **352**:172–188.

[14] Hansbo, P. and Larson, M.G. Finite element modeling of a linear membrane shell problem using tangential differential calculus. *Comp. Methods Appl. Mech. Engrg.* (2014) **270**:1–14.

[15] Fries, T.-P. and Schöllhammer, D. A unified finite strain theory for membranes and ropes. *Comput. Methods Appl. Mech. Engrg.* (2020) **365**:113031

[16] Fries, T.-P. Higher-order surface FEM for incompressible Navier-Stokes flows on manifolds. *Internat. J. Numer. Methods Fluids* (2018) **88**:55-78

[17] Jankuhn, T., Olshanskii, M. and Reusken, A. Incompressible fluid problems on embedded surfaces: Modeling and variational formulations. *Interface Free Bound* (2018) **20**:353-377

[18] Huges, T.J.R, Cottrell, J.A. and Bazilevs, Y. Isogeometric analysis: CAD, finite elements, NURBS, exact geometry and mesh refinement. *Comp. Methods Appl. Mech. Engrg.* (2005) **194**:4135–4195.

[19] Cottrell, J.A., Hughes, T.J.R. and Bazilevs, Y. *Isogemometric analysis: Toward integration of CAD and FEA.* Wiley, (2009).

[20] Gurtin, M.E. and Murdoch, I.A. A continuum theory of elastic material surfaces. *Arch. Ration. Mech. Anal.* (1975) **57**:291-323.